CPU vs RAM in the Issue of *ab initio* Simulations of Doped Hafnium Oxide for RRAM and FRAM

Timofey V. Perevalov[1] iD *, Damir R. Islamov*[1,2] iD

Atomic and electronic structure of dopped HfO_2 is studied using first principle simulations. The 96- and 324-atom supercell are used to simulate impurity density in the range of 2–6.3 mol.% that is used in real electronic memory devices. The optimal spatial configurations of impurity atoms with an oxygen vacancy are found. It is shown that there are no defect levels in the band gap dopped HfO_2 with the optimal structures. The electronic structure of additional neutral oxygen vacancy in HfO_2 is equivalent to that of neutral oxygen vacancy in pure HfO_2. An increase in the size of a supercell predictably leads to an increase in the need for computing resources. At the same time, the need for RAM is growing faster than for CPU power. Doping HfO_2 with Al/La/Y with concentration of up to 6.2 mol.% has negligible effect on the electronic structure of neutral oxygen vacancies.

Keywords: supercomputer, high performance computing, paradigm of structural calculations, parallelism, quantum chemistry, memristor.

Introduction

Promising candidates for the role of universal memory, which combines the advantages of Random Access Memory (RAM), Hard Drive Disks and Flash memory, are resistive (RRAM) and ferroelectric (FRAM) memories based on hafnium oxide (HfO_2) [16, 22]. In a HfO_2-based RRAM, the resistive switching between states of different resistance is carried out when exposed to an external electric field due to the formation/breaking of a conductive filament. In the HfO_2-based FRAM, the information storage is supported by the dielectric polarization in the ferroelectric layer. The switching of polarization is carried out through the application of an external electric field. The performance of such a device is ensured by the ferroelectric phase stabilization in HfO_2 films. It is known that doping HfO_2 with various metals, such as Al, La and Y, leads to the increased performance of RRAM and FRAM cells: reduced forming voltage, increased memory window and increased number of reprogramming cycles [2, 9, 10, 18, 21, 23]. The mechanisms by which the dopant influences the characteristics of RRAM and FRAM have not been established yet. This problem can be solved using first principle simulations within the density functional theory (DFT). However, to do this, first of all, it is necessary to establish the atomic structure of doped HfO_2. Despite a fairly large number of studies on this issue, they are all limited to the use of model structures, the correctness of which has not been proven yet [3, 6, 13–15, 20, 24–26].

The complexity of the task is determined by two factors. First of all, the use of HfO_2 supercells with the replacement of two Hf atoms by impurity atoms and an oxygen vacancy necessary for the charge compensation of the system, necessitates the search for the most probable (energetically favorable) spatial position of three defects in a supercell. It should be clarified that this particular HfO_2 doped with Al, La, Y model structure is the most popular and justified, since the valency of the considered impurities is one lower than that of hafnium. This requires considering a huge number of nonequivalent defect configurations. Thus, for the 96-atomic supercell of the

[1]Rzhanov Institute of Semiconductor Physics, Siberian Branch of the Russian Academy of Sciences, Novosibirsk, Russian Federation

[2]Novosibirsk State University, Novosibirsk, Russian Federation

monoclinic phase (m-) HfO$_2$ (with 32 metal atoms and two types of oxygen vacancies), which is mostly used in calculations, obtained by the $2 \times 2 \times 2$ translation of a primitive 12-atomic cell, it is necessary to calculate $C_{32}^2 \times 2 = 992$ configurations. In the vast majority of existing studies, the authors limit themselves to considering the defect configurations in which a pair of impurity atoms is in close proximity to oxygen vacancy.

The second difficulty is that to simulate HfO$_2$ with an impurity concentration of about 2 mol.%, corresponding to the best characteristics of real RRAM and FRAM elements based on doped HfO$_2$, it is necessary to use supercells of 324 atoms (obtained by a symmetric translation of a $3 \times 3 \times 3$ primitive cell). The use of a 96-atom supercell corresponds to the simulation of an overestimated impurity concentration of 6.25 mol.%. The correctness of the results obtained for 324-atom supercells was not verified due to the need to use a lot of computing resources. It is important to note that despite the absence of serious difficulties in calculating of this scale systems for standard DFT, to correctly reproduce the electronic structure and, in particular, the position of defect levels in the band gap, it is necessary to use a significantly more resource-intensive DFT with hybrid exchange-correlation functionals. This, in turn, requires significantly more computational resources.

Thus, the purpose of this work is to study the atomic and electronic structure of HfO$_2$ doped with Al, La and Y at low concentrations. The study includes, firstly, determining the optimal atomic structures of HfO$_2$ doped with Al, La and Y from the point of view of energy efficiency; secondly, studying the influence of the supercell size on the resulting optimal structure and, thirdly, simulations the electronic structure of additional oxygen vacancies in the found structures. Additionally, the problem was formulated as studying the influence of the supercell size on the reproducibility of the calculation results of the atomic and electronic structure of defect complexes.

The article is organized as follows. Section 1 is devoted to structures under study and calculation methods of electronic structure of structure defects in the studied electronic systems. In Section 2 we discuss obtained results. Subsection 2.1 is devoted to the description of the atomic and electronic structures of HfO$_2$ supercells with mutual arrangement of the impurity atoms and oxygen vacancies. In Subsection 2.2 the required computing resources for the simulations of 96- and 324-atom HfO$_2$ supercells are discussed and compared. Conclusion summarizes the study and points directions for further work.

1. Methods

The simulations were carried out within the DFT in the approximation of a periodic 3D supercell, with a plane-wave basis and optimized norm-conserving Vanderbilt pseudopotentials [7, 8] using the Quantum ESPRESSO (QE) software package [4, 5]. Two types of exchange-correlation functionals were used: PBEsol to calculate structural relaxation and B3LYP to calculate the electronic spectrum of optimal HfO$_2$:X structures (X in one of Al, Y or La). The simulation was carried out for the m-HfO$_2$ ($P2_1/c$) phase. This phase is the most stable and closest in physical properties to amorphous HfO$_2$, and is also observed in real HfO$_2$ films used in RRAM and FRAM elements. The optimal structures of HfO$_2$:X were found by calculating all possible nonequivalent configurations of the arrangement of oxygen vacancy and a pair of impurity atoms at the Hf substitution position in 96-atom supercells from which configurations with the minimum total energy of the system were selected. For 324-atom supercells, the search for optimal structures was carried out by finding the optimal position of the first impurity atom

at a fixed position of the oxygen vacancy, and then of the second one. The oxygen vacancy, in this case, is a structural element of HfO_2:Al/Y/La providing a charge compensation for the impurity, and, for convenience, is further referred to as a structural vacancy (V_O). The calculations used the plane waves cutoff energy $80\,Ry$, the Fock exchange operator cutoff energy $100\,Ry$, the k-point grid $2 \times 2 \times 2$, the Fock operator point grid $1 \times 1 \times 1$, the exact exchange fraction for B3LYP 0.175 (which provides the m-HfO_2 bandgap value of $5.8\,eV$) and the total energy convergence threshold $10^{-4}\,Ry$. In the found HfO_2:X structures, the optimal position of the additional oxygen vacancy with the minimum formation energy (hereinafter denoted $V_O^{'}$) was found by calculating and analyzing all possible positions in the supercell. The spatial distributions of atoms and defects in HfO_2:X supercells were visualized using the XCrySDen program [11, 12]. The used computing resources and memory distributions were extracted from QE reports.

The energy of $V_O^{'}$ formation (E_{form}) was calculated using the formula:

$$E_{form} = E(V_O^{'}) - E_p + \mu(O), \qquad (1)$$

where $E(V_O^{'})$ is the energy of the HfO_2:X supercell with neutral $V_O^{'}$; E_p is the energy of the 'perfect' supercell without $V_O^{'}$; $\mu(O)$ is the chemical potential on an oxygen atom O. For the convenience of comparing the results with literature data, the $\mu(O)$ value was taken equal to half the total energy of the O_2 molecule in the triplet state, which corresponds to the oxygen-enriched limit.

2. Results and Discussions

2.1. Atomic and Electronic Structures

After calculating all possible spatial configurations of the Al/La/Y atom pair position in supercells of 96- and 324-atoms with oxygen vacancy V_O, optimal structures with the lowest total energy were found (Fig. 1). The spread of the total energy of supercells with different defect configurations is about $3\,eV$, while the structure closest in energy differs from the optimal one by about $0.4\,eV$. It was established that the features of the atomic structure obtained for 96 and 324-atomic supercells coincide. It is obvious that further decrease in the impurity concentration due to an increase in the supercell size will not lead to changes in the optimal mutual arrangement of the impurity atoms and V_O. Thus, the use of a 96-atom supercell is sufficient to reproduce the main features of the relative arrangement of impurity atoms in m-HfO_2.

In all structures, V_O is 3-coordinated. In HfO_2:La and HfO_2:Y, the impurity atoms are spaced from each other at approximately $6\,\text{Å}$, with one of the impurity atoms located close to V_O at a distance of $r \approx 2\,\text{Å}$, and the second – at $r \approx 4.1\,\text{Å}$ from V_O. For La/Y near V_O the coordination number is 6, for the second La/Y it is 7. It is noteworthy that, the total energy of HfO_2:La and HfO_2:Y supercells with an optimal structure is lower (by more than $0.4\,eV$), compared with the total energy of non-optimal structures, that were used in calculations in the works of various authors previously [6, 13–15, 20, 25]. The optimal structure of HfO_2:Al, on the contrary, meets this assumption: V_O is located between the Al atoms at $r \approx 2.3\,\text{Å}$ from each Al, while the Al atoms are relatively close to each other ($r \approx 4.5\,\text{Å}$). It is probably energetically unfavorable for La and Y atoms to be too close to each other due to their large ionic radius compared to the Hf one: $R_{Hf} = 0.85\,\text{Å}$, $R_{La} = 1.17\,\text{Å}$, $R_Y = 1.06\,\text{Å}$ [19]. In HfO_2:Al, a pair of Al atoms might be close to each other due to a small Al ionic radius ($R_{Al} = 0.68\,\text{Å}$).

(a) 96-at. m-HfO$_2$:Al   (b) 96-at. m-HfO$_2$:La   (c) 96-at. m-HfO$_2$:Y

(d) 324-at. m-HfO$_2$:Al   (e) 324-at. m-HfO$_2$:La   (f) 324-at. m-HfO$_2$:Y
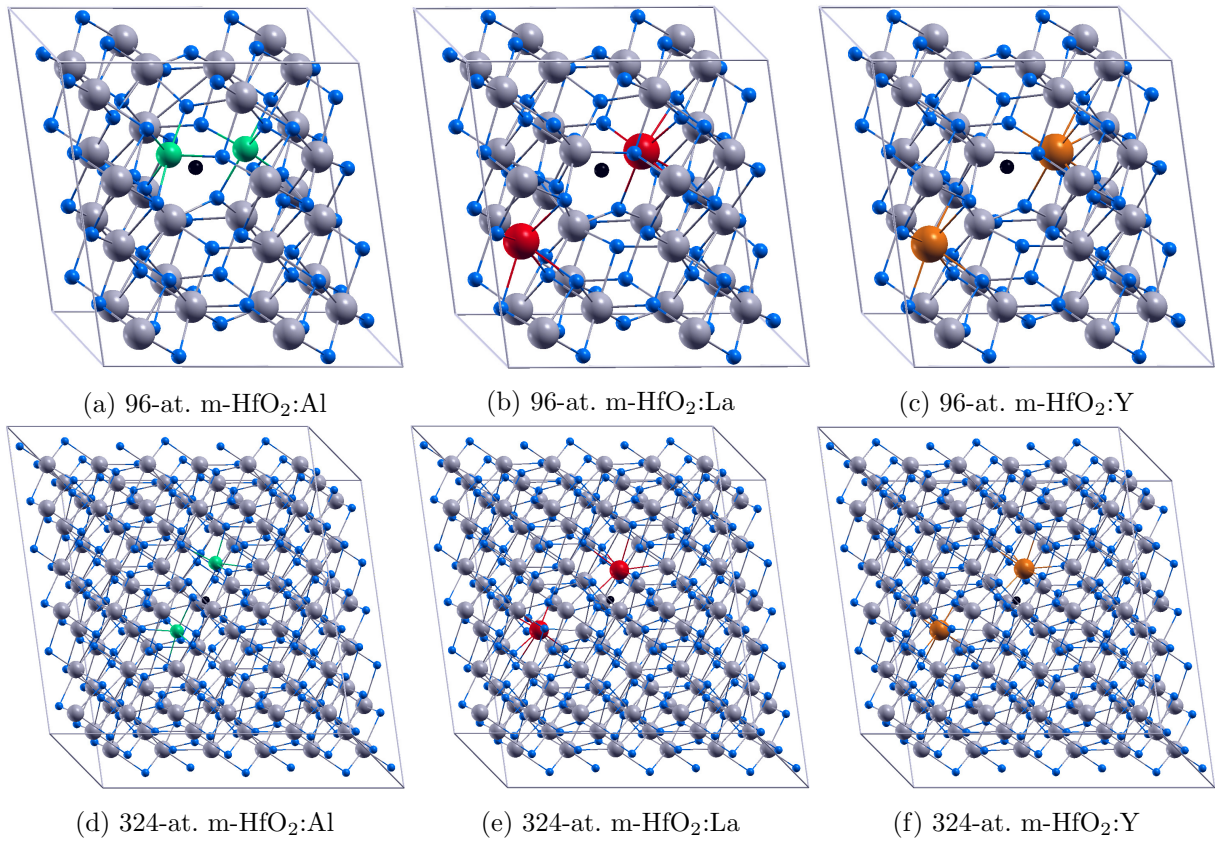
Figure 1. Supercells of 96- and 324-atoms of the optimal m-HfO$_2$:Al, m-HfO$_2$:La and m-HfO$_2$:Y structures. Gray color balls are Hf, blue ones are O, green ones are Al, red ones are La and black ones represent O vacancies (removed O atoms)
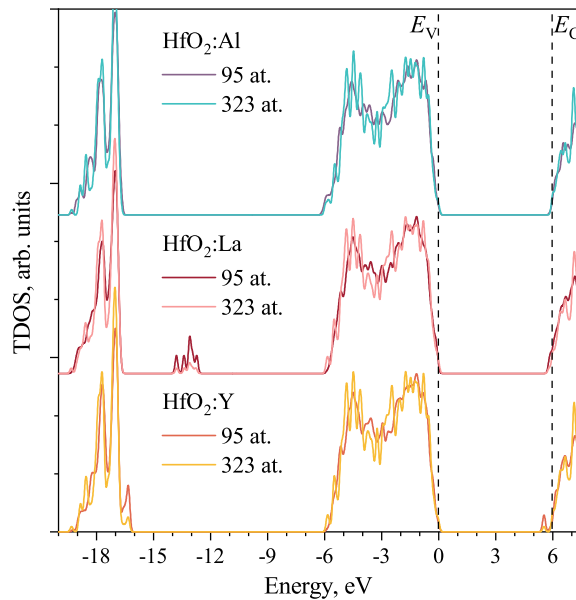

Figure 2. TDOS spectra calculated for the optimal HfO$_2$:Al, HfO$_2$:La and HfO$_2$:Y structures. Zero energy corresponds to the valence band top E_V

The total density of states (TDOS) spectra calculated for HfO$_2$ doped with Al, La and Y with concentrations of 6.25 mol.% and 2 mol.% show that the band gap of all oxides is empty

(Fig. 2). This result is consistent with the experimental data, according to which doping HfO_2 with lanthanum does not change the bandgap E_g [17]. In contrast, the TDOS spectra for non-optimal structures have an empty level with a depth of about $1\,eV$ [13, 15]. In doped HfO_2, as well as in pure HfO_2, $E_g = 5.85\,eV$, which is close to the experimental value $E_g = 5.7\,eV$ [1]. In the case of doping with La, a subband with an energy of about $14\,eV$ below the valence band top E_V is formed predominantly by La$5p$ orbitals, which can be seen in the TDOS spectrum.

It was established that the optimal position of an additional oxygen vacancy V_O' in 95- and 323-atomic supercells of HfO_2:Al, HfO_2:La and HfO_2:Y, with the minimal E_{form}, is near one of the impurity atoms. As a result, in HfO_2:La and HfO_2:Y, both impurity atoms become 6-coordinated. For HfO_2:La and HfO_2:Y, the V_O-V_O' distance is $5.50\,\text{Å}$, and for HfO_2:Al it is $3.13\,\text{Å}$. The E_{form} of V_O' weakly depends on the value of the considered defect density and is approximately $0.2\,eV$ less than the E_{form} of the vacancy in undoped HfO_2. Thus, doping HfO_2 with Al/La/Y facilitates the generation of new oxygen vacancies in the oxide. Recently, the opposite results have been obtained, however, when the non-optimal structures of doped HfO_2 were simulated [20, 25].
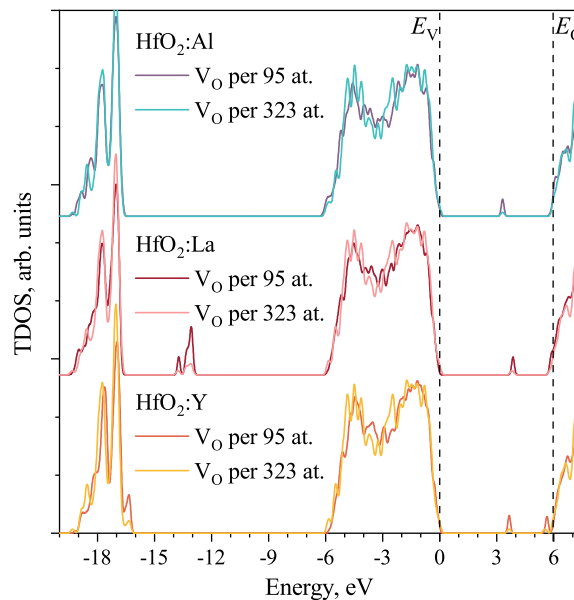

Figure 3. TDOS spectra calculated for HfO_2, HfO_2:Al and HfO_2:La structures with additional V_O'. Zero energy corresponds to the valence band top E_V

In doped HfO_2, a neutral V_O' forms a level filled with two electrons just above the middle of the bandgap, as shown in Fig. 3. The position of this level, firstly, weakly depends on the type of dopant (any of Al, La or Y); secondly, it does not depend on the impurity concentration, and, thirdly, it is close to that for a neutral oxygen vacancy in undoped HfO_2. Thus, one can conclude that doping HfO_2 with Al/La/Y with a concentration of up to $6.2\,mol.\%$ has a negligible effect on the electronic structure of neutral oxygen vacancies.

2.2. Required Computing Resources

The required computing resources for the simulations of 96- and 324-atom HfO_2 supercells are given in Tab. 1. As the cell size increased, the complexity of the problem increased about 3.4 times. At the same time, CPU time increased about 6–7 times, while the memory require-

ments increased more significantly, about 8 times. The memory is mainly used to store data from exact-exchange (EXX) integrals within hybrid functional, wave-functions and β-functions of non-local pseudopotentials. The needs for EXX and β-function data increased 7 times and that is close to the total growth of using RAM resources. Note that the data volume for reducing matrices to the diagonal shape has increased more than 13 times.

Table 1. Resource consumption per calculation

	96 at.	324 at.	$324/96 = 3.375$
CPU, core×hour	~ 120	~ 720	~ 6–7
RAM, GB	~ 50–60	~ 450–470	~ 7–9
Wavefunctions, GB	$\sim 9,6$	$\sim 18,4$	~ 2
EXX, GB	~ 35	~ 253	~ 7
Structure factor, GB	~ 0.04	~ 0.08	~ 2
Local pseudopotentials	~ 0	~ 0	$-$
Nonlocal pseudopotentials (beta functions), GB	~ 2.4	~ 16	~ 7
Nonlocal pseudopotentials (Q functions), GB	~ 0.5	~ 0.5	~ 1
Charge density and potentials, GB	~ 0.2	~ 0.2	~ 1
Charge density in initialization, GB	~ 0.05	~ 0.05	~ 1
Grid vectors, GB	~ 0.05	~ 0.1	~ 2
Iterative diagonalization (matrices), GB	~ 0.03	~ 0.4	~ 13
Iterative diagonalization (scalar products), GB	~ 0.4	~ 5	~ 13
Iterative diagonalization (charge density), GB	~ 1.2	~ 7.5	~ 6
Wavefunctions in initialization, GB	~ 2	~ 13	~ 7

Conclusion

This work is devoted to the thorough study on the atomic and electronic structure of HfO_2 doped with aluminum, lanthanum and yttrium. The simulation was carried out for two impurity concentrations, covering the actual range of doping density of films in real electronic devices. Two types of oxygen vacancies are considered, namely, the oxygen vacancy involved in compensating the impurity charge (V_O) and the additional oxygen vacancy ($V_O^{'}$). It was established that, in the optimal structure of the doped oxide, La and Y atoms tend to distance themselves from each other at about 6 Å. Just one of the La/Y atom is located near V_O, while both Al atoms are located near one common V_O and the distance between Al is about 4 Å. It was established that the features of the atomic structure obtained for 96 and 324-atomic supercells coincide. The data obtained for HfO_2:La and HfO_2:Y arouse doubts as for all the results previously published on this topic. It was found that there are no defect levels in the bandgap of HfO_2:Al, HfO_2:La and HfO_2:Y with the optimal structures. The formation of additional neutral vacancy $V_O^{'}$ in HfO_2 near Al, Y or La atoms is facilitated, compared to the formation of V_O in undoped HfO_2. The electronic structure of $V_O^{'}$ in HfO_2:Al, HfO_2:La and HfO_2:Y is equivalent to that of neutral V_O in pure HfO_2.

Increasing the size of a supercell leads to an increase in the need for computing resources. At the same time, the need for RAM is growing faster than for the CPU power. Since doping HfO_2

with Al/La/Y with concentration of up to $6.2\,\mathrm{mol.\%}$ has a negligible effect on the electronic structure of neutral oxygen vacancies, 96-atomic supercells exhibit all features of m-HfO_2.

Acknowledgements

References

1. Balog, M., Schieber, M., Michman, M., Patai, S.: Chemical vapor deposition and characterization of HfO_2 films from organo-hafnium compounds. Thin Solid Films 41, 247–259 (1977). `https://doi.org/10.1016/0040-6090(77)90312-1`

2. Dai, Y., Zhao, Y., Wang, J., *et al.*: First principle simulations on the effects of oxygen vacancy in HfO_2-based RRAM. AIP Advances 5, 017133 (2015). `https://doi.org/10.1063/1.4906792`

3. Gao, B., Zhang, H.W., Yu, S., *et al.*: Oxide-based RRAM: Uniformity improvement using a new material-oriented methodology. In: 2009 Symposium on VLSI Technology, pp. 30–31 (2009).

4. Giannozzi, P., Andreussi, O., Brumme, T., *et al.*: Advanced capabilities for materials modelling with Quantum ESPRESSO. Journal of Physics: Condensed Matter 29(46), 465901 (2017). `https://doi.org/10.1088/1361-648x/aa8f79`

5. Giannozzi, P., Baroni, S., Bonini, N., *et al.*: QUANTUM ESPRESSO: a modular and opensource software project for quantum simulations of materials. Journal of Physics: Condensed Matter 21(39), 395502 (2009). `https://doi.org/10.1088/0953-8984/21/39/395502`

6. Gu, C., Ang, D.S.: Impact of lanthanum on positive-bias temperature instability – insight from first-principles simulation. ECS Transactions 53(3), 193–204 (2013). `https://doi.org/10.1149/05303.0193ecst`

7. Hamann, D.R.: Optimized norm-conserving vanderbilt pseudopotentials. Physical Review B 88, 085117 (2013). `https://doi.org/10.1103/physrevb.88.085117`

8. Hamann, D.R.: Erratum: Optimized norm-conserving vanderbilt pseudopotentials [phys. rev. b 88, 085117 (2013)]. Physical Review B 95, 239906 (2017). `https://doi.org/10.1103/physrevb.95.239906`

9. He, R., Wu, H., Liu, S., *et al.*: Ferroelectric structural transition in hafnium oxide induced by charged oxygen vacancies. Physical Review B 104, L180102 (2021). `https://doi.org/10.1103/physrevb.104.l180102`

10. Islamov, D.R., Perevalov, T.V.: Effect of oxygen vacancies on the ferroelectric $Hf_{0.5}Zr_{0.5}O_2$ stabilization: DFT simulation. Microelectronic Engineering 216, 111041 (2019). `https://doi.org/10.1016/j.mee.2019.111041`

11. Kokalj, A.: XCrySDen – a new program for displaying crystalline structures and electron densities. Journal of Molecular Graphics & Modelling 17(3-4), 176–179 (1999). `https://doi.org/10.1016/s1093-3263(99)00028-5`

12. Kokalj, A.: Computer graphics and graphical user interfaces as tools in simulations of matter at the atomic scale. Computational Materials Science 28, 155–168 (2003). `https://doi.org/10.1016/s0927-0256(03)00104-6`

13. Leitsmann, R., Plänitz, P., Nadimi, E., Öttking, R.: Oxygen related defects and the reliability of high-k dielectric films in FETs. In: 2013 International Semiconductor Conference Dresden - Grenoble (ISCDG). pp. 1–4. IEEE (2013). `https://doi.org/10.1109/iscdg.2013.6656327`

14. Materlik, R., Künneth, C., Falkowski, M., *et al.*: Al-, Y-, and La-doping effects favoring intrinsic and field induced ferroelectricity in HfO_2: A first principles study. Journal of Applied Physics 123, 164101 (2018). `https://doi.org/10.1063/1.5021746`

15. Nadimi, E., Öttking, R., Plänitz, P., *et al.*: Interaction of oxygen vacancies and lanthanum in Hf-based high-k dielectrics: an *ab initio* investigation. Journal of Physics: Condensed Matter 23(36), 365502 (2011). `https://doi.org/10.1088/0953-8984/23/36/365502`

16. Park, M.H., Lee, Y.H., Mikolajick, T., *et al.*: Review and perspective on ferroelectric HfO_2-based thin films for memory applications. MRS Communications 8, 795–808 (2018). `https://doi.org/10.1557/mrc.2018.175`

17. Perevalov, T.V., Prosvirin, I.P., Suprun, E.A., *et al.*: The atomic and electronic structure of $Hf_{0.5}Zr_{0.5}O_2$ and $Hf_{0.5}Zr_{0.5}O_2$:La films. Journal of Science: Advanced Materials and Devices 6(4), 595–600 (2021). `https://doi.org/10.1016/j.jsamd.2021.08.001`

18. Pešić, M., Fengler, F.P.G., Larcher, L., *et al.*: Physical mechanisms behind the field-cycling behavior of HfO_2-based ferroelectric capacitors. Advanced Functional Materials 26, 4601–4612 (may 2016). `https://doi.org/10.1002/adfm.201600590`

19. Shannon, R.D.: Revised effective ionic radii and systematic studies of interatomic distances in halides and chalcogenides. Acta Crystallographica Section A 32(5), 751–767 (1976). `https://doi.org/10.1107/s0567739476001551`

20. Umezawa, N., Shiraishi, K., Sugino, S., *et al.*: Suppression of oxygen vacancy formation in Hf-based high-k dielectrics by lanthanum incorporation. Applied Physics Letters 91, 132904 (2007). `https://doi.org/10.1063/1.2789392`

21. Voronkovskii, V.A., Aliev, V.S., Gerasimova, A.K., Islamov, D.R.: Influence of HfO_x composition on hafnium oxide-based memristor electrical characteristics. Materials Research Express 5(1), 016402 (2018). `https://doi.org/10.1088/2053-1591/aaa099`

22. Zahoor, F., Zulkifli, T.Z.A., Khanday, F.A.: Resistive random access memory (RRAM): an overview of materials, switching mechanism, performance, multilevel cell (mlc) storage,

modeling, and applications. Nanoscale Research Letters 15(1), 1–26 (2022). `https://doi.org/10.1186/s11671-020-03299-9`

23. Zalyalov, T.M., Islamov, D.R.: The influence of the dopant concentration on the ferroelectric properties and the trap density in $Hf_{0.5}Zr_{0.5}O_2$:La films during endurance cycling. In: 2022 IEEE 23rd International Conference of Young Professionals in Electron Devices and Materials (EDM). pp. 48–51. IEEE (2022). `https://doi.org/10.1109/edm55285.2022.9855130`

24. Zhang, H., Gao, B., Yu, S., *et al.*: Effects of ionic doping on the behaviors of oxygen vacancies in HfO_2 and ZrO_2: A first principles study. In: 2009 International Conference on Simulation of Semiconductor Processes and Devices. pp. 1–4. IEEE (2009). `https://doi.org/10.1109/sispad.2009.5290225`

25. Zhao, L., Liu, J., Zhao, Y.: Systematic studies of the effects of group-III dopants (La, Y, Al, and Gd) in $Hf_{0.5}Zr_{0.5}O_2$ ferroelectrics by *ab initio* simulations. Applied Physics Letters 119, 172903 (2021). `https://doi.org/10.1063/5.0066169`

26. Zhou, Y., Zhang, Y.K., Yang, Q., *et al.*: The effects of oxygen vacancies on ferroelectric phase transition of HfO_2-based thin film from first-principle. Computational Materials Science 167, 143–150 (2019). `https://doi.org/10.1016/j.commatsci.2019.05.041`